J. Membrane Biol. 82, 25–40 (1984)

The Journal of
Membrane Biology
© Springer-Verlag 1984

Apical Sodium Entry in Split Frog Skin: Current-Voltage Relationship

Joel DeLong and Mortimer M. Civan
Departments of Physiology and Medicine, University of Pennsylvania School of Medicine, Philadelphia, Pennsylvania 19104

Summary. Apical Na^+ entry into frog skin epithelium is widely presumed to be electrodiffusive in nature, as for other tight epithelia. However, in contrast to rabbit descending colon and *Necturus* urinary bladder, the constant field equation has been reported to fit the apical sodium current (I_{Na})-membrane potential (ψ^{mc}) relationship over only a narrow range of apical membrane potentials or to be inapplicable altogether. We have re-examined this issue by impaling split frog skins across the basolateral membrane and examining the current-voltage relationships at extremely early endpoints in time after initiating pulses of constant transepithelial voltage. In this study, the rapid transient responses in ψ^{mc} were completed within 0.5 to 3.5 msec. Using endpoints to 1 to 25 msec, the Goldman equation provided excellent fits of the data over large ranges in apical potential of 300 to 420 mV, from approximately −200 to about +145 mV (cell relative to mucosa). Split skins were also studied when superfused with high serosal K^+ in order to determine whether the I_{Na}-ψ^{mc} relationship could be generated purely by transepithelial measurements. Under these conditions, the basolateral membrane potential was found to be -10 ± 3 mV (cell relative to serosa, mean ± SE), the basolateral fractional resistance was greater than zero, and the transepithelial current was markedly and reversibly reduced. For these reasons, use of high serosal K^+ is considered inadvisable for determining the I_{Na}-ψ^{mc} relationship, at least in those tissues (such as frog skin) where more direct measurements are technically feasible. Analysis of the I_{Na}-ψ^{mc} relationships under baseline conditions provided estimates of intracellular Na^+ concentration and of apical Na^+ permeability of 9 to 14 mM and of $\sim 3 \times 10^{-7}$ cm · sec^{-1}, respectively, in reasonable agreement with estimates obtained by different techniques.

Key Words Goldman equation · intracellular Na^+ concentration · apical Na^+ permeability · high serosal K^+ · membrane potential · electrodiffusive channels

Introduction

Sodium transport through epithelial cells proceeds in two steps: passive entry from the mucosal medium across the apical membrane, and active extrusion across the basolateral membrane by the sodium-potassium exchange pump. At least some tissues appear to regulate transepithelial sodium movement to a large extent by varying apical sodium permeability (e.g., Lichtenstein & Leaf, 1965; Lewis, Eaton & Diamond, 1976; Civan, 1983). In studying net sodium movement, it is therefore essential to measure both the electrical and chemical driving forces and the sodium permeability (P_{Na}^{ap}) across the apical plasma membrane.

In principle, the apical membrane potential (ψ^{mc}, cell relative to mucosal medium), the intracellular sodium activity (a_{Na}^{c}), and P_{Na}^{ap} can all be measured simply by intracellular and transepithelial electrical recordings during the course of trains of constant voltage or constant current pulses. This approach is simple and rapid, but is based on a number of premises. First, the junction and tip potentials of the exploring micropipette must be minimized, with or without correction for the residual junction potential. Second, the transcellular sodium current is taken to be the amiloride-sensitive transepithelial current. Third, permeability estimated by fitting the constant field equation (Goldman, 1943) to the apical sodium current-voltage relationship (I_{Na}^{mc}-ψ^{mc}) is generally presumed to reflect Na^+ movement through aqueous channels even when the experimental fit is satisfactory over only a limited voltage range. Fourth, the apical permeability so derived is clearly relevant only to conductive pathways across the membrane; to the extent that electroneutral mechanisms support apical Na^+ entry, P_{Na}^{ap} should be less than the apical sodium permeability measured by tracer fluxes.

Despite the limited documentation of certain of these premises, direct or indirect measurements of the I_{Na}^{mc}-ψ^{mc} relationship in several epithelial tissues have provided useful estimates of a_{Na}^{c} and P_{Na}^{ap} (Fuchs, Larsen & Lindemann, 1977; Palmer, Edelman & Lindemann, 1980; Frömter, Higgins & Gebler, 1981; Schultz, Thompson & Suzuki, 1981; Thompson, Suzuki & Schultz, 1981; Li et al., 1982; Palmer et al., 1982; Thomas et al., 1983). This

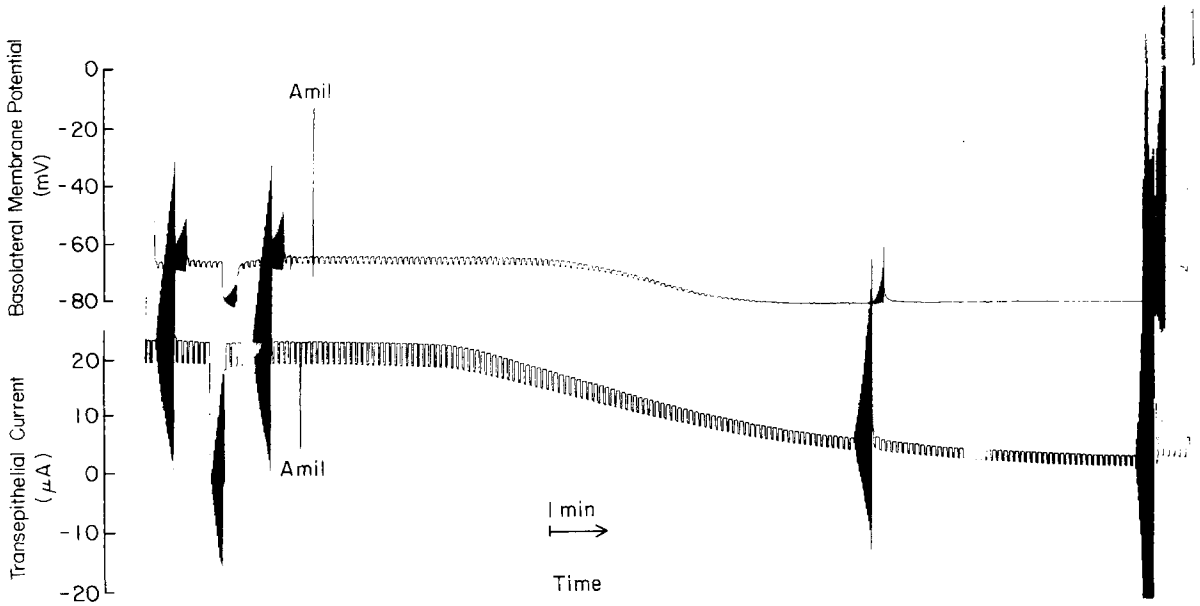

Fig. 1. Intracellular and transepithelial recordings during impalement of a single cell. The upper trace is the difference in electrical potential between the exploring micropipette and the serosal reference solution before, during and after impalement. The lower trace is the transepithelial current. The tissue was voltage-clamped alternately to 0 and to +10 mV (serosa positive to mucosa) except when trains of voltage pulses were applied. In the second pulse train, the holding transepithelial voltage was shifted from 0 to +60 mV. At the time indicated "Amil," the mucosal surface was superfused with Ringer's solution containing 10^{-4} M amiloride; the basolateral fractional resistance, and short-circuit current subsequently fell, and the magnitudes of the intracellular potential and transepithelial resistance rose, as expected. In the final pulse train, a computer error caused a series of incorrectly large voltage pulses to be applied, terminating the experiment. The records of Figs. 1 and 6 were taken during the same impalement; the record of Fig. 10*A* was obtained with the same preparation

approach was first taken by Fuchs et al. (1977), who introduced a further experimental simplification. They reasoned that if, indeed, the basolateral membrane behaved as a potassium electrode (Koefoed-Johnsen & Ussing, 1958), matching the intracellular potassium activity with a high serosal potassium activity should abolish the potential and minimize the resistance of the basolateral membrane. For such a "depolarized" preparation, the I_{Na}^{mc}-ψ^{mc} relationship of the apical membrane could be determined simply from transepithelial measurements of current and voltage, alone.

As will be considered in the Discussion, published reports have been in disagreement whether or not the apical sodium current-voltage relationship can be rigorously measured using depolarized epithelia. In the specific case of the frog skin, it has even been unclear whether or not intracellular recordings can be fit by the constant field equation (Helman, 1981, his Fig. 6; Tang & Helman, 1982). In the present study, we have re-examined these questions, using two experimental modifications. First, split frog skin rather than whole skin has been used in order to eliminate possible contributions of the skin glands (Carasso et al., 1971; Civan et al., 1983), to minimize the importance of impalement-induced shunts (Higgins, Gebler & Frömter, 1977), and to avoid any technical complication associated with the passage of the micropipette tips through the *stratum corneum*. Second, in order to reduce the significance of voltage-induced membrane changes, we have studied the apical sodium current-voltage relationship at short intervals after the onset of voltage pulses. The endpoints chosen have ranged from 25 msec to as low as 1 msec. At the lower end of this range, the endpoints of the present study have been at least an order of magnitude shorter than those used in any of the published studies cited above.

Materials and Methods

Abdominal skins were excised from doubly pithed frogs (*Rana pipiens pipiens*) obtained from West Jersey Biological Supply (Wenonah, N.J.). The underlying corium was removed by the enzymatic method of Fisher, Erlij and Helman (1980). The split epithelium was then mounted serosal side up between the two halves of a Lucite® chamber (Delong & Civan, 1978), exposing 1.9 cm^2 for experimental study. The serosal and mucosal surfaces were separately superfused with solutions, usually at a flow rate of 3 to 4 ml · min^{-1}.

Table 1. Intracellular and transepithelial electrical values (with and without mucosal amiloride) for three short-circuited split skins bathed in chloride-containing Ringer's solution

Condition	ψ_o^{mc}(mV)	f_o^{ap}	R_T(k$\Omega \cdot cm^2$)	I_{SC}($\mu A \cdot cm^{-2}$)
Before amiloride	−71 ± 2	0.92 ± 0.02	3.8 ± 0.9	11 ± 3
After amiloride	−87 ± 5	0.967 ± 0.004	8 ± 3	1.9 ± 0.7

The standard Ringer's solution (R) contained (mM): Na^+ 118.2; K^+ 118.2; K^+ 3.4; Ca^{2+} 0.9; Cl^- 117.2; HCO_3^- 2.3; HPO_4^{2-} 1.8; $H_2PO_4^-$ 0.3; the pH was 7.5 to 7.6 and osmolality 223 to 228 mOsm. A sodium sulfate Ringer's solution (NaS-R) and a potassium sulfate Ringer's solution (KS-R) similar to those described by Fuchs et al. (1977) were also used. The NaS-R consisted of (mM): Na^+ 99.1; K^+ 3.4; Ca^{2+} 2.0; SO_4^{2-} 50.0; gluconate 2.0; HEPES (N-2-hydroxyethylpiperazine-N'-2-enthanesulfonic acid and salt) 5.0; the pH was 7.4 and osmolality 130 to 132 mOsm. The KS-R was identical to the sodium sulfate Ringer's solution except for the equimolar replacement of all Na^+ by K^+.

The split skins were impaled across the basolateral membranes with single-barrelled micropipettes drawn from omega-dot capillary glass tubing (Glass Co. of America, Millville, N.J.) and similar to those used previously (DeLong & Civan, 1983*a*). The filling solution was 0.5 M KCl solution in order to reduce the rate of release of saline into the cell during prolonged impalements (Nelson, Ehrenfeld & Lindemann, 1978; Fromm & Schultz, 1981). Criteria for acceptability of penetrations of frog skin have been discussed elsewhere (Civan et al., 1983; DeLong & Civan, 1983*a*). In each case, the intracellular potential was stable for at least 1 min, and usually for far longer periods of time.

The transepithelial potential (ψ^{ms}, serosa positive to mucosa) was measured and clamped alternately to 0 mV for 7.7 sec and to 10 mV for 4.3 sec. The basolateral membrane potential (ψ^{sc}, cell relative to serosa), the total transepithelial current (I_T, positive current from mucosa to serosa) and transepithelial potential were continuously monitored and displayed on a storage oscilloscope. ψ^{sc} and I_T were also continuously recorded on a dual-pen chart recorder. At appropriate intervals, the baseline voltage clamping was interrupted in order to apply a train of voltage pulses across the epithelium. During the course of the pulse train, ψ^{ms} was changed and then restored to the baseline value, usually of 0 mV. In most cases, the pulse pattern consisted of 12 pairs of alternately positive and negative pulses, whose magnitude increased by 20 mV in successive steps. Each pulse lasted 30.72 msec; the entire series of pulses was completed in approximately 1 min.

The transepithelial current and basolateral membrane potential were continuously displayed on a strip chart recorder. During delivery of pulse patterns, the transepithelial current, basolateral membrane potential and transepithelial potential were digitally recorded through a multiplexed 12-bit ADC controlled by an LSI-11/03 microcomputer. The three channels were scanned 512 times with the first 128 scans occurring during pulse-off, the middle 256 scans during pulse-on and the final 128 scans during pulse-off. Between pulses, the data were recorded on floppy disk. Voltage pulses were generated by a 12-bit bipolar DAC. Data reduction was performed by the LSI-11 and the reduced data were displayed on a printer, graphics monitor and/or plotter.

Further experimental details concerning the biological and electrophysiological manipulations are available in previous publications from this laboratory (Civan et al., 1983; DeLong & Civan, 1983*a*,*b*).

Results

An example of the raw data obtained during the course of an experiment is provided in Fig. 1. After measuring the baseline electrophysiological values, pulse trains were executed at a holding voltage of 0 mV, except for the second series of pulses (obtained with a holding voltage of 60 mV). After the application of mucosal amiloride, the short circuit (I_{sc}) fell, ψ_o^{sc} hyperpolarized, and R_T and the apical fractional resistance (f_o^{ap}) both increased. The basolateral (f_o^{bl}) and apical fractional resistances are calculated as the ratio of the voltage change across each membrane to the total transepithelial polarization. The subscript "*o*" is included to indicate that the calculation is carried out for data points obtained near $\psi^{ms} = 0$ mV. The prolonged interval between addition of, and response to, amiloride in Fig. 1 reflected the low perfusion rate used at the time of impalement in order to reduce the likelihood of dislodging the micropipette tip by changing the mucosal superfusing solution. The transient change in mucosal hydrostatic pressure did, in fact, generally dislodge the micropipette tip, even when this precaution was taken.

Complete and technically satisfactory electrophysiologic data were obtained with three split skins bathed with chloride-containing Ringer's solutions. For these three preparations, the values of ψ_o^{mc}, f_o^{ap}, R_T and I_{SC} before and after superfusing with 1.2 to 10.0 × 10^{-4} M mucosal amiloride are presented in Table 1. These and the subsequent data to be reported are presented as means ± SE unless otherwise stated.

Figure 2 presents ψ^{mc}, I_T and ψ^{ms} before, during and after clamping the transepithelial potential to eight separate values (±20, ±60, ±120 and ±220 mV) from a holding voltage of 0 mV. The rapid transient responses of the transepithelial and apical membrane potentials are complete after about 0.5 msec. The detectable capacitative effects on ψ^{mc} were also very brief in the other skins studied in chloride-Ringer's solution (Figs. 3*b* and *c*) and sul-

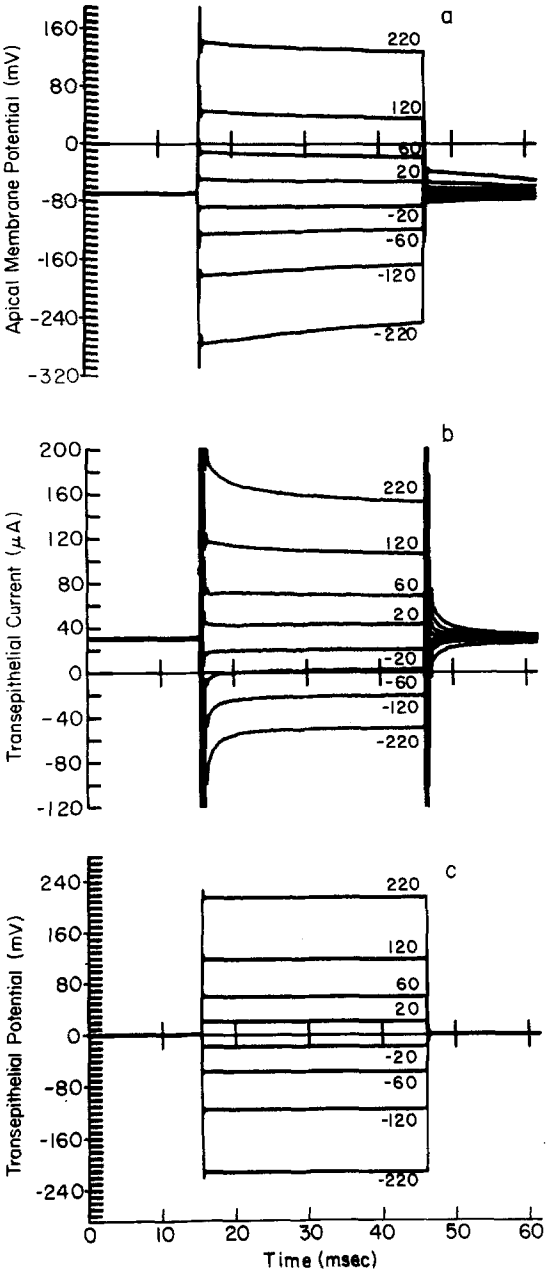

Fig. 2. Time courses of apical membrane potential (ψ^{mc}), transepithelial current (I_T) and transepithelial voltage (ψ^{ms}) before, during and after clamping the tissue to $\psi^{ms} = \pm 20$, ± 60, ± 120 and ± 220 mV under baseline conditions. The transepithelial holding voltage was 0 mV. The records of Figs. 2, 3*b*, 5, 7–9 and 11 have been obtained from the same preparation

fate-Ringer's solution (Figs. 3*d* and *e*). Small later shifts in membrane potential with time can be observed in most of the traces of Fig. 3 following step changes in ψ^{ms} to 100 mV. However, these slower time-dependent changes do not seem to reflect membrane capacitative effects for at least two reasons: (i) After the first few milliseconds, the membrane polarizations *decline* slightly with time towards their prepulse values (ψ_o^{mc}). In contrast to these slight later relaxations towards their baseline values, the deflections of the apical membrane potentials ($|\psi^{mc} - \psi_o^{mc}|$) display larger initial *increases* with time in response to the depolarizations of Figs. 3*d* and 3*e*. We identify these initial time-dependent increases as capacitative in nature, and the later time-dependent falls as reflecting changes in apical fractional resistance and/or polarizations within the tissue. (ii) The slow time-dependent reduction in $|\psi^{mc} - \psi_o^{mc}|$ is abolished by amiloride (Fig. 5). Since the basolateral membrane conductance far exceeds that of the apical membrane, amiloride would be expected to have little or no change on the time constant (τ) of the apical membrane potential given by Eq. (11A) of the Appendix and reproduced below.

Measured from the initial time courses of the transepithelial currents following step polarizations in ψ^{ms} to 100 mV, the time constants for the five preparations of Fig. 3 ranged from 1.11 to 1.62 msec, with a mean of 1.35 ± 0.09 msec. As considered in the Discussion, these response times are somewhat faster than anticipated on the basis of the simple equivalent circuit of Fig. 4 examined by Schultz et al.[1] and analyzed in the Appendix.

The time constant (τ) for capacitative changes in the transepithelial current and apical membrane potential can be calculated from Eq. (11A) of the Appendix:

$$1/\tau \equiv [1/(C_a + C_b)][(1/R_a) + (1/R_b)] \qquad (11A)$$

where the subscripts "*a*" and "*b*" refer to the apical and basolateral membranes, respectively, and the circuit elements are defined in Fig. 4. The apical (R_a) and basolateral (R_b) membrane resistances can be estimated by first calculating the total transcellular transepithelial resistance (R^c) as the reciprocal of the amiloride-sensitive transepithelial conductance. Then,

$$R_a = f_o^{ap} R^c \qquad (1)$$

$$R_b = (1 - f_o^{ap}) R^c. \qquad (2)$$

For the five preparations of Fig. 3, the mean values of R_a and R_b were 13 ± 2 kΩ · cm² and 1.4 ± 0.4 kΩ · cm², respectively. Assuming apical (C_a) and basolat-

[1] Schultz, S.G., Thompson, S.M., Hudson, R., Thomas, S.R., Suzuki, Y. Electrophysiology of *Necturus* urinary bladder: II. Time-dependent current-voltage relations of the basolateral membranes. (*submitted for publication*)

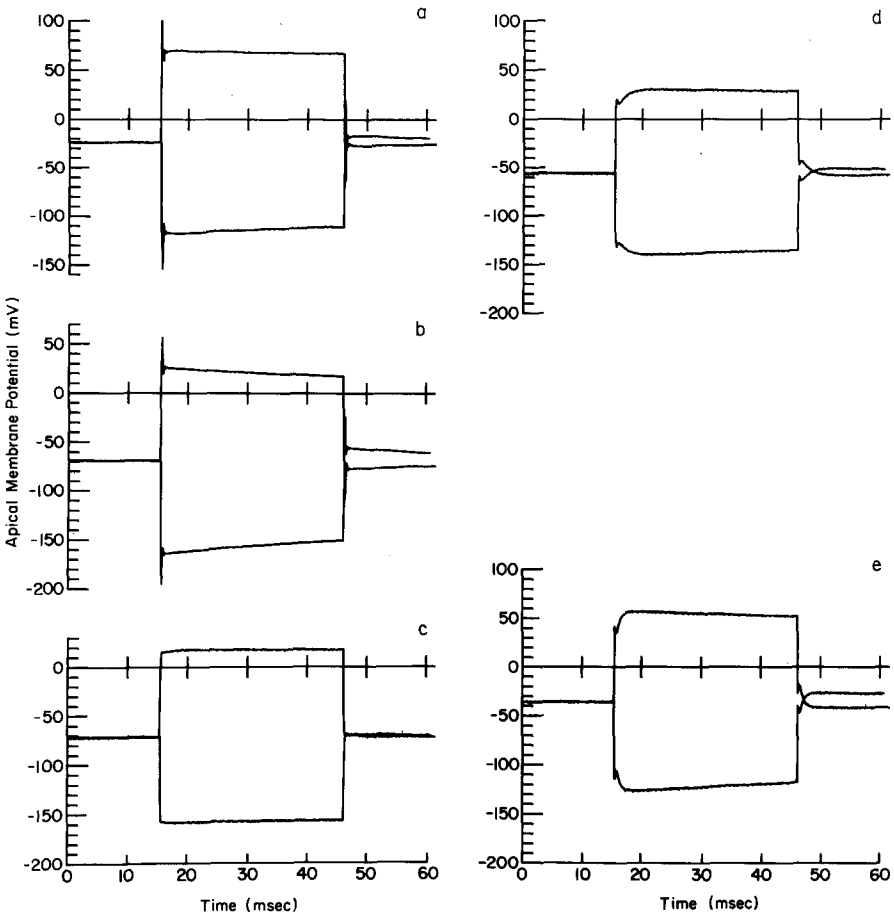

Fig. 3. Time courses of ψ^{mc} for five different tissues before, during and after clamping ψ^{ms} to ± 100 mV. The preparations of panels *a*, *b* and *c* were studied in chloride Ringer's solution, while those of *d* and *e* were superfused with sulfate Ringer's solution. The transient responses of Figs. *a–c* appear to be complete within a msec, while those of *d* and *e* are complete within 3.5 and 2.5 msec, respectively

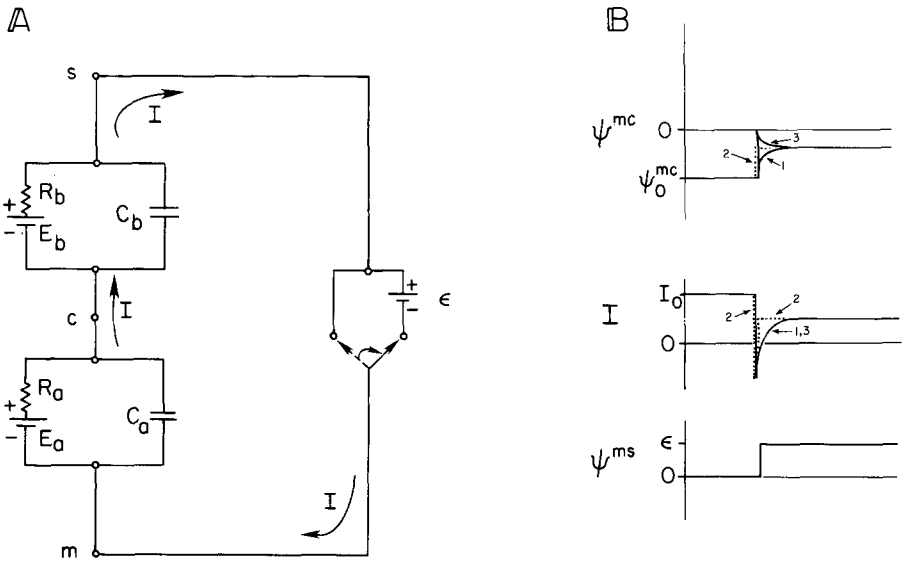

Fig. 4. Equivalent circuit and predicted time courses of apical membrane potential, transcellular current and transepithelial potential before and after increasing transepithelial potential from 0 to ε. The symbols are defined in the Appendix

eral (C_b) membrane capacitances of 1 $\mu F \cdot cm^{-2}$, the values of τ predicted by Eq. (11A) above are 0.7 to 4.6 msec, with a mean of 2.6 ± 0.7 msec for the five split skins of Fig. 3. The mean value for the ratio of measured-to-calculated estimates of τ is 0.8 ± 0.3. The capacitative transients are considered in greater detail in the Discussion.

Following the addition of amiloride, the time

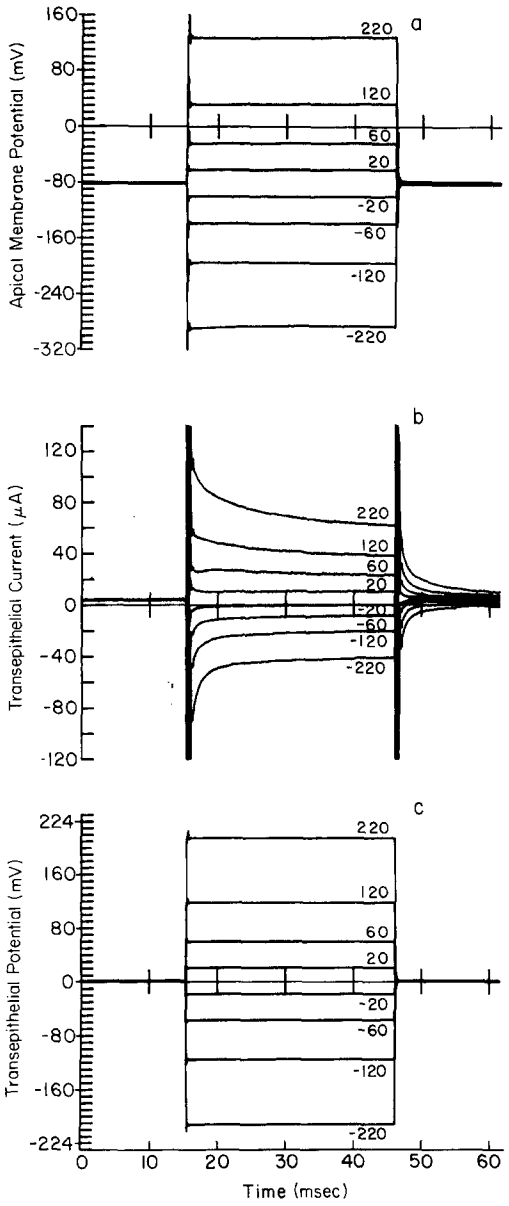

Fig. 5. Time courses of ψ^{mc}, I_T and ψ^{ms} in presence of 10^{-3} M amiloride

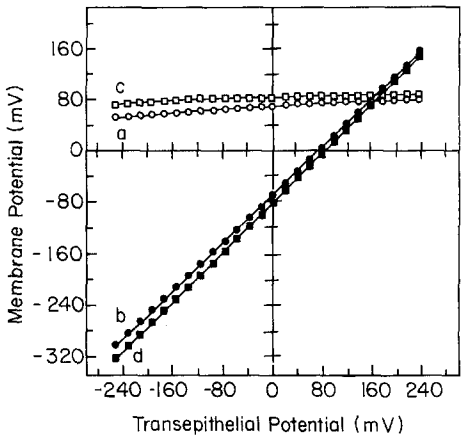

Fig. 6. Basolateral (ψ^{cs}; *a*, *c*) and apical (ψ^{mc}; *b*, *d*) membrane potentials as a function of transepithelial potential. The data were obtained from the impalements of a single cell before (*a*, *b*) and after (*c*, *d*) superfusing the mucosal surface with 10^{-4} M amiloride. The measurements were made 8 msec after initiating each voltage pulse

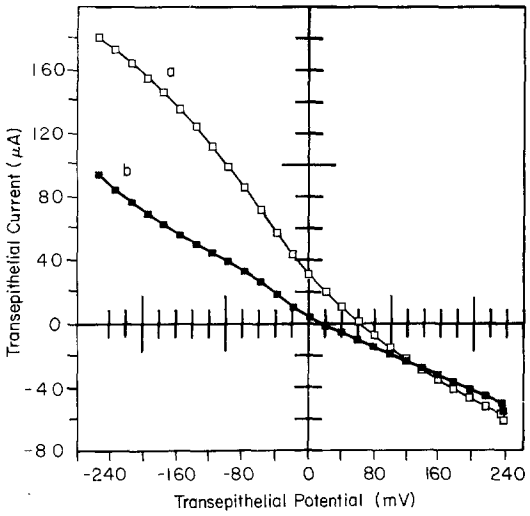

Fig. 7. Transepithelial current as a function of transepithelial voltage before (*a*) and after (*b*) superfusing the mucosal surface with 10^{-3} M amiloride at an endpoint of 8 msec

courses of ψ^{mc}, I_T and ψ^{ms} (Fig. 5) were qualitatively similar to those elicited under control conditions (Fig. 2). The major differences were: (i) the more squarewave nature of the ψ^{mc} trace during the course of the transepithelial voltage waveform, and (ii) the reduced magnitude of I_T.

Figure 6 presents the basolateral and apical membrane potentials as functions of transepithelial potential in the presence and absence of amiloride, using an endpoint of 8 msec. The values presented are the means calculated for the 5-data points recorded in the 0.6 msec-interval beginning 8 msec after initiating the pulses; a similar averaging procedure was used for each of the other endpoints chosen. Because of the high apical fractional resistance, the curvilinear nature of the dependence of membrane potential on trasepithelial potential is far more readily appreciated from the ψ^{cs} than from the ψ^{cs} than from the ψ^{mc} trace. Amiloride increased f_o^{ap} from a baseline value of 0.945 to 0.974. In this and all other estimates of f_o^{ap} and f_o^{bl} in the present study, the values were calculated from measurements of ψ^{sc} and ψ^{ms} 8 msec after initiating transepithelial pulses of +20 and −20 mV. We consider measure-

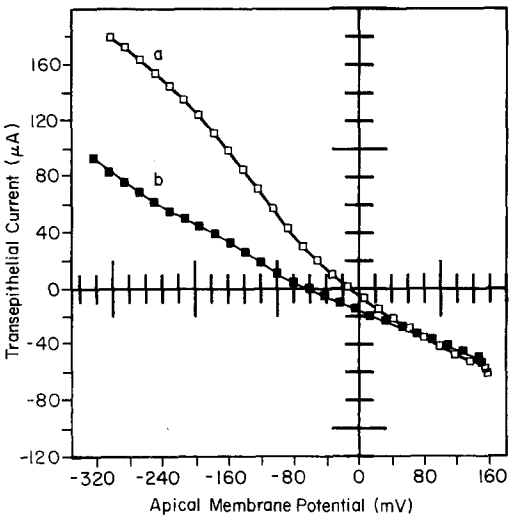

Fig. 8. Transepithelial current as a function of apical membrane potential before (*a*) and after (*b*) mucosal application of 10^{-3} M amiloride at an endpoint of 8 msec

ments of apical membrane resistance at this early endpoint to be more reliable indices of membrane properties than the more commonly used later endpoints in time; the latter measurements are more strongly affected by transient effects not directly reflecting the baseline membrane properties (reviewed by Weinstein et al., 1980).

The dependence of transepithelial current upon transepithelial potential and upon apical membrane potential are presented in Figs. 7 and 8, respectively. The apical sodium current I_{Na} at a given value of ψ^{ms} has been defined as the fall in I_T produced by amiloride at that transepithelial voltage. The calculated values of I_{Na} at an endpoint of 8 msec have been displayed as a function of apical membrane potential (prior to adding amiloride) in Fig. 9. The data points of panels 9*a–e* are identical. The panels differ only in the values of the parameters of the Goldman equation (Goldman, 1943) used to construct the solid lines. The equation may be expressed as:

$$I_{Na} = -\left[\frac{P_{Na}^{ap} F^2 \psi^{mc}}{RT}\right]\left[\frac{c_{Na}^{m} - c_{Na}^{c} e^{[\psi^{mc}F/(RT)]}}{1 - e^{[\psi^{mc}F/(RT)]}}\right]; \psi^{mc} \neq 0 \quad (3)$$

$$I_{Na} = P_{Na}^{ap} F(c_{Na}^{m} - c_{Na}^{c}); \psi^{mc} = 0 \quad (4)$$

where F is the Faraday constant, R is the perfect gas constant, T is the absolute temperature, and c_{Na}^{m} and c_{Na}^{c} are the Na^+ concentrations in the mucosal medium and cell, respectively. All of the parameters of Eqs. (3) and (4) are known or measured with the exception of c_{Na}^{c} and P_{Na}^{ap}. As demonstrated by

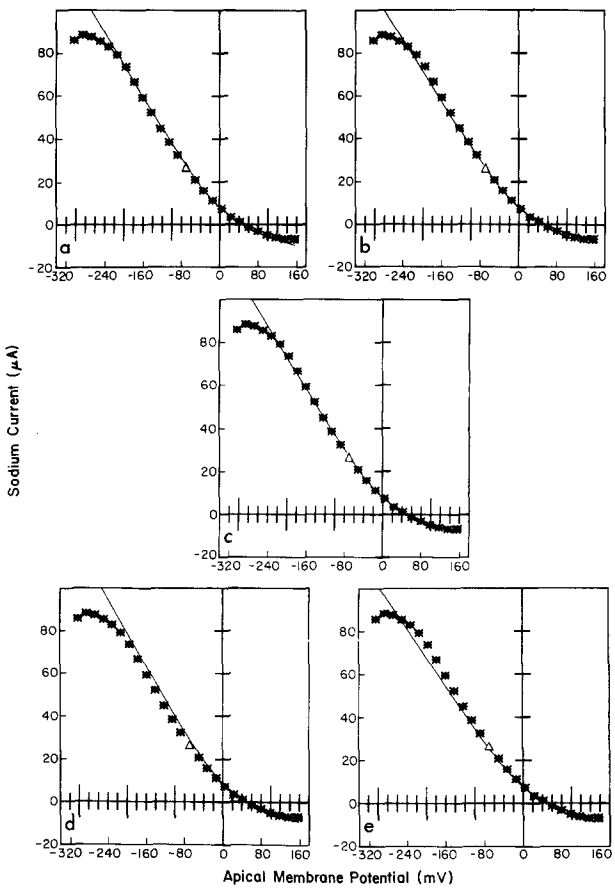

Fig. 9. Fit of constant field equation to sodium current-voltage relationship of apical membrane. The data points in each of the 5 panels are the same. Only the parameters of the Goldman equation have been changed in order to demonstrate that even slight deviations from the best choice of parameters (9*c*) significantly worsen the degree of fit. The values of intracellular sodium concentration (in mM) and apical membrane permeability for Na^+ (in $cm^3 \cdot sec^{-1}$) are: (*a*) 19.6, 8.4×10^{-7}; (*b*) 14.9, 8.0×10^{-7}; (*c*) 17.4, 8.2×10^{-7}; (*d*) 17.4, 8.8×10^{-7}; and (*e*) 17.4, 7.6×10^{-7}. Except for a single data point, all of the measurements are the means of the 5 data points obtained during the 0.6 msec beginning 8 msec after initiating the voltage pulses; the single exception (symbolized by a triangle in this and succeeding Figures) is the point reflecting the mean values of sodium current and apical membrane potential measured at the holding transepithelial potential (of zero) just prior to initiating each voltage pulse

Fig. 9*c* setting $c_{Na}^{c} = 17.4$ mM and $P_{Na}^{ap} = 8.2 \times 10^{-7}$ $cm^3 \cdot sec^{-1}$ leads to an excellent fit of the data over nearly a 400-mV range in ψ^{mc} from −231 mV to 156 mV. This and subsequent fits have been done by eye. As illustrated by the other four panels of Fig. 9, changing the choice of assumed values even slightly results in a significant worsening of the fit. In order to better permit the reader to judge the excellence of fit, the data of Fig. 9*c* are also expressed in digital form in Table 2. Over the range in ψ^{mc} from −231 to 156 mV, the maximum deviation (δI_{Na}) of calculated

Table 2. Tabular presentation of agreement between calculated and measured values of sodium current as a function of apical membrane potential

ψ^{ms}(mV)	ψ^{mc}(mV)	$I_T(\mu A)$		$I_{Na}(\mu A)$		
		Before amiloride	After amiloride	Measured	Calculated	Diff.
−174.0	−231.4	145.0	62.2	82.8	84.5	1.7
−154.7	−213.4	134.7	55.7	79.1	78.0	−1.1
−135.3	−195.1	123.6	50.1	73.6	71.3	−2.3
−115.8	−177.2	111.1	44.7	66.5	64.8	−1.7
−96.4	−159.8	98.4	39.2	59.2	58.5	−0.7
−77.0	−141.7	84.9	32.8	52.1	51.9	−0.2
−57.5	−123.4	71.1	26.4	44.7	45.4	0.7
−38.0	−105.3	56.9	18.5	38.4	39.0	0.6
−18.7	−87.8	42.7	10.3	32.3	33.0	0.7
0.9	−69.2	30.2	4.0	26.1	26.8	0.7
20.5	−50.8	19.5	−1.2	20.7	21.1	0.4
39.6	−33.1	10.2	−5.5	15.8	16.0	0.2
59.2	−14.5	0.7	−10.4	11.2	11.2	0.0
78.6	4.0	−7.4	−14.7	7.3	7.2	−0.1
98.2	22.8	−15.6	−19.1	3.5	3.7	0.2
117.5	41.5	−22.5	−23.7	1.2	1.0	−0.2
137.0	60.4	−29.3	−27.9	−1.4	−1.3	0.1
156.3	79.5	−35.5	−32.3	−3.2	−3.1	0.1
175.7	98.4	−41.7	−36.7	−4.9	−4.6	0.3
195.3	117.0	−47.3	−41.3	−6.1	−5.9	0.2
214.6	135.7	−52.4	−45.6	−6.8	−7.1	−0.3
234.0	154.7	−57.0	−50.1	−7.0	−8.2	−1.2
236.1	156.3	−61.6	−55.0	−6.6	−8.3	−1.7

The data have been obtained from the same set of results presented graphically in Fig. 9*C*. The measured values of I_{Na} have been taken to be the differences in total transepithelial currents (I_T) before and after amiloride. The calculated values have been obtained using Eq. (3), and setting $P_{Na}^{ap} = 8.2 \times 10^{-7}$ cm^3 · sec^{-1} and $c_{Na}^{c} = 17.4$ mM.

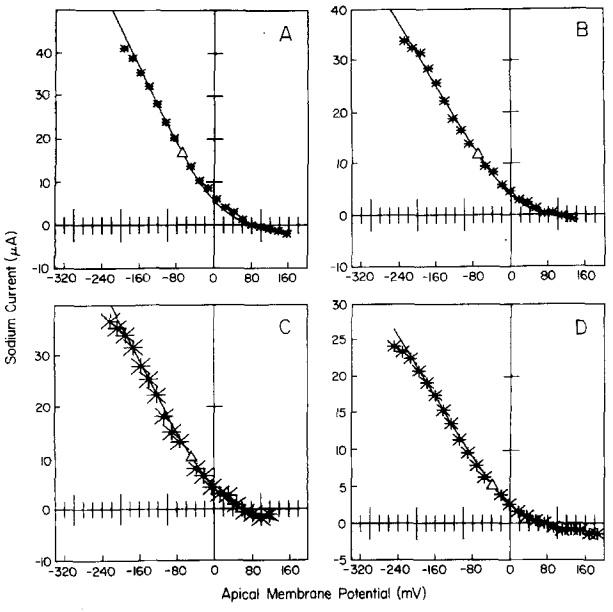

Fig. 10. Fits of constant field equation to data obtained from four different tissues superfused with chloride- and sulfate-containing Ringer's solutions. In each case, the data were obtained 8 msec after initiating each voltage step, and the skins were bathed with identical solutions on the two surfaces. (*A*) R, constant field equation calculated for $c_{Na}^{c} = 5.6$ mM and $P_{Na}^{ap} = 5.1 \times 10^{-7}$ cm^3 · sec^{-1}. (*B*) R, $c_{Na}^{c} = 5.8$ mM, $P_{Na}^{ap} = 3.5 \times 10^{-7}$ cm^3 · sec^{-1}. (*C*) NaS-R, $c_{Na}^{c} = 11.3$ mM, $P_{Na}^{ap} = 4.0 \times 10^{-7}$ cm^3 · sec^{-1}. (*D*) NaS-R, $c_{Na}^{c} = 7.7$ mM, $P_{Na}^{ap} = 4.8 \times 10^{-7}$ cm^3 · sec^{-1}

from measured values of I_{Na} was 2.3 μA. The standard deviation of δI_{Na} for the N measurements, given by $\left[\sum_i (\delta I_{Na})_i^2/(N-2)\right]^{1/2}$, was 0.96 μA; this value is only 1% of the total change in I_{Na} of 89.8 μA over the range of agreement.

In the four additional experiments of Fig. 3 (termed "complete experiments"), sufficient technically satisfactory data were obtained in order to construct similar $I_{Na} - \psi^{mc}$ plots. These data are presented in Fig. 10, using an endpoint of 8 msec. Figs. 10*A* and *B* were obtained from skins bathed with R, while the skins of Figs. 10*C* and *D* were superfused with NaS-R. In the least satisfactory fit (that of Fig. 10), we consider the fit to be good over a range of values of ψ^{mc} of 340 mV. In the remaining panels, the fit is excellent over voltage ranges of 300 to 420 mV.

Figure 11 presents the apical sodium current-voltage relationship as a function of pulse duration. The solid curves of Fig. 11*a–f* are identical plots of the constant field equation, taking $c_{Na}^{c} = 17.4$ mM and $P_{Na}^{ap} = 8.2 \times 10^{-7}$ cm^3 · sec^{-1}. This single choice of values provided a reasonably good fit of the data over the entire range of end points examined of 1 to 25 msec. However, the earliest and latest of the data sets can be better fit by a slightly different choice of parametric values, as illustrated by Figs.

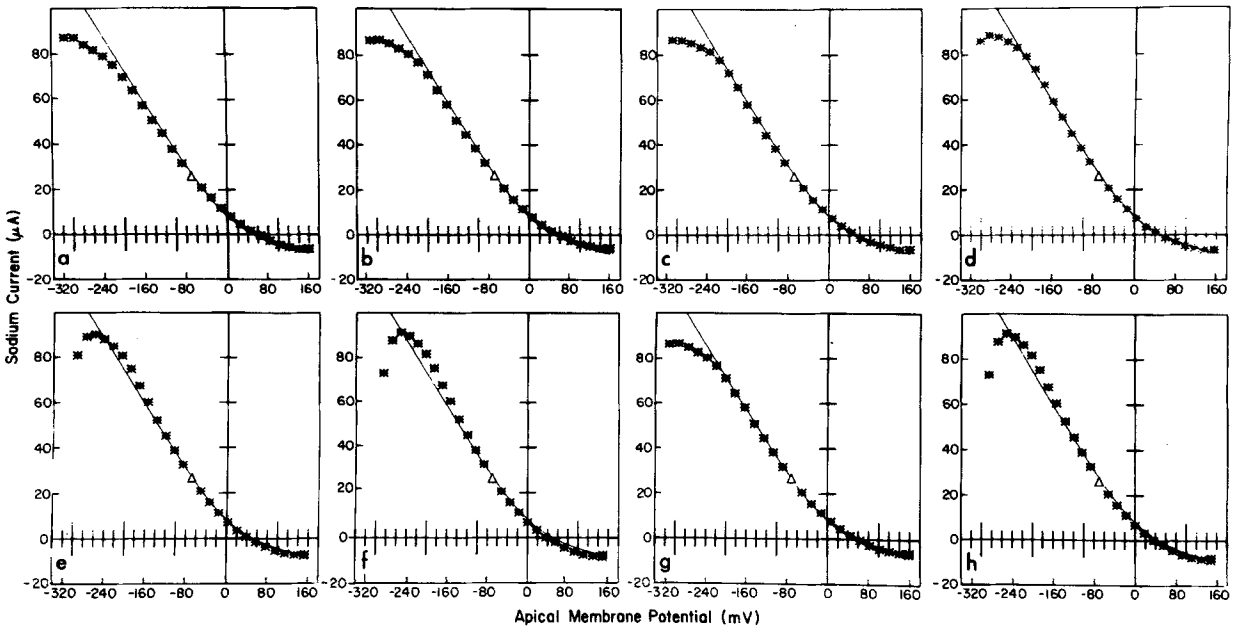

Fig. 11. Sodium current-voltage relationship of apical membrane as a function of time after initiating voltage steps. In contrast to Fig. 7, each of the 6 panels 11*a–f* includes a plot of the Goldman equation based on the same values of intracellular sodium concentration and apical sodium permeability of 17.4 mM and 8.2×10^{-7} cm^3 · sec^{-1}, respectively. However, the times T (after initiating the voltage step) at which the data points were calculated were 1, 2, 4, 8, 16 and 25 msec for 11*a–f*, respectively. Although the same Goldman equation can be used to fit all 6 curves reasonably well, the earliest and latest time points can be fit slightly better by the two theoretical curves of 11*g* and 11*h*, respectively: (*g*)τ = 2 msec, c^c_{Na} = 14.9 mM, and $P^{ap}_{Na} = 8.0 \times 10^{-7}$ cm^3 · sec^{-1}; (*h*)τ = 25 msec, c^c_{Na} = 19.6 mM, and $P^{ap}_{Na} = 8.4 \times 10^{-7}$ cm^3 · sec^{-1}

Table 3. Calculated values of intracellular Na^+ concentration (c^c_{Na}) and apical Na^+ permeability (P^{ap}_{Na}) as a function of time (T) after initiating voltage steps

Parameter	Junction potential (mV)	T(msec)					
		1	2	4	8	16	25
c^c_{Na}(mM)	0	8 ± 5(3)	7 ± 2(5)	9 ± 2(5)	10 ± 2(5)	9 ± 2(5)	10 ± 3(5)
	7.3	9 ± 5(3)	9 ± 3(5)	12 ± 4(5)	12 ± 3(5)	12 ± 4(5)	14 ± 4(5)
P^{ap}_{Na}(10^{-7}cm^3 · sec^{-1})	0	6 ± 1(3)	4.9 ± 0.8(5)	5.0 ± 0.8(5)	5.0 ± 0.8(5)	5.2 ± 0.8(5)	5.2 ± 0.9(5)
	7.3	5 ± 1(3)	4.7 ± 0.8(5)	4.8 ± 0.8(5)	4.9 ± 0.8(5)	4.9 ± 0.8(5)	5.0 ± 0.9(5)

The calculations have been performed assuming a junction potential between micropipette and intracellular fluids of 0 and 7.3 mV (filling solution relative to cell). The numbers in parentheses are the numbers of preparations whose I_{Na}-ψ^{mc} relationship could be fit to the Goldman equation at each volume of τ.

11*g* and 11*h*. From the values used in Fig. 11*a–f*, 11*g* and 11*h* the uncertainty in estimating c^c_{Na} from the calculated fits for this preparation is taken to be about ±2 to 3 mM and in P^{ap}_{Na} to be approximately $\pm 0.2 \times 10^{-7}$ cm^3 · sec^{-1}. Although the estimates of c^c_{Na} tended to be slightly higher at the end of the voltage pulses than at the beginning, the effect was small and not statistically significant. The values of the means ± SE for the two parameters, obtained from all five complete experiments, are presented in Table 3.

Table 3 provides a summary of the reduced data calculated in two ways. In one case, the junction potential (ϕ) between the filling solution of the micropipette and the intracellular fluids is assumed to be negligible. However, experimental results obtained with *Chironomus* salivary glands (Palmer & Civan, 1977) and frog skin (DeLong & Civan, 1983*a*), and theoretical considerations suggest that ϕ is significantly larger than 0. Therefore, the data have also been fit to the Goldman equation, assuming the value estimated by DeLong and Civan for frog skin of ϕ = 7.3 mV (micropipette relative to cell).

One of the aims of the present work has been to determine whether application of high serosal po-

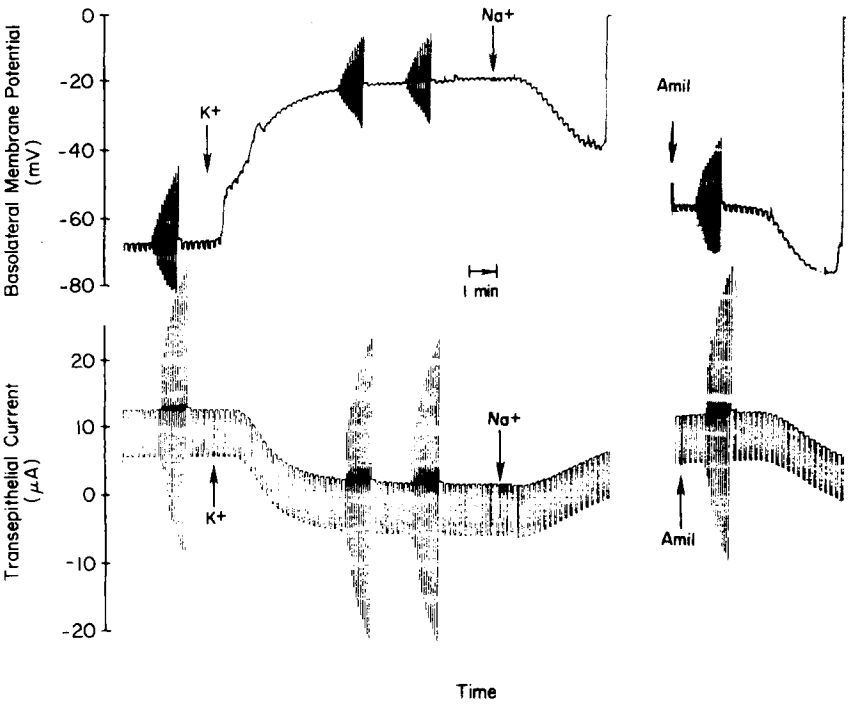

Fig. 12. Intracellular and transepithelial recordings during the course of transiently replacing serosal Na^+ with K^+, and during the course of adding mucosal amiloride. The records were obtained from the same preparation as those of Figs. 3*d*, 10*c* and 13. The mucosal medium was NaS-R throughout the experiment

tassium permits the valid accumulation of data similar to those of Figs. 9–11 and Table 2 purely from transepithelial measurements, as originally suggested by Fuchs, Larsen and Lindemann (1977). Figure 12 illustrates the protocol used. Split skins were first incubated in Na_2SO_4-Ringer's solution (NaS-R), and baseline measurements obtained. The serosal superfusate was then replaced by KS-R, in which K^+ was substituted for all the serosal Na^+. Pulse trains were again applied across the epithelium. After 10 to 16 min in contact with high serosal K^+, the serosal surface was again superfused with NaS-R.

In order to rigorously document the intracellular position of the micropipette when superfusing with serosal NaS-R, an additional criterion for impalement acceptability was imposed. Measurements of ψ_o^{sc} under these conditions were included only if the micropipette tip remained in place while NaS-R was restored as the superfusing fluid and if ψ_o^{sc} clearly hyperpolarized after the replacement of serosal Na^+. One experiment met this additional minimal criterion for acceptability. In another five experiments, more complete intracellular recordings (like that of Fig. 12) were obtained, in which both the depolarization by high serosal K^+ and the subsequent hyperpolarization by restoring serosal Na^+ were measured during impalement of a single cell. We have considered this added criterion to be important. Otherwise, basolateral impalements of cells with highly depolarized membrane potentials and low basolateral fractional resistances might not be recognized as *bona fide* intracellular impalements. Of the six successful experiments conducted in NaS-R, sufficient added information was accumulated in two skins to permit generation of the I_{Na}-ψ^{mc} relationships of Figs. 10*C* and 10*D*.

Table 4 presents a summary of some of the results obtained with sulfate-Ringer's solutions. The most striking baseline observation was the relatively low membrane potential of -47 ± 5 mV in the short-circuited state. Five of the skins displayed values of ψ_o^{mc} ranging from -33 to -51 mV. In one preparation, ψ_o^{mc} was -66 mV, the only value to fall within the range of membrane potentials we commonly observed using chloride-Ringer's solution. Replacement of serosal Na^+ with K^+ caused a prompt, marked and reversible reduction in membrane potential and in short-circuit current. High serosal K^+ also produced a reversible increase in apical fractional resistance and a reversible fall in total transepithelial resistance in each of the six experiments. Thus, even by nonparametric analysis, each of these K^+-induced changes is significant at the 0.02 probability level.

The magnitude of the depolarization produced by high serosal K^+ was variable. In three experiments, ψ_o^{mc} was reduced to -3 to -7 mV. In two other experiments, however, ψ_o^{mc} was -18 to -19 mV. In the final experiment, ψ_o^{mc} was slightly higher than the mean of -10 ± 3 mV.

Although the basolateral fractional resistance f_o^{bl}

Table 4. Effects of replacing K^+ for Na^+ in serosal medium

Ringer's solution	ψ_o^{mc}(mV)	f_o^{ap}	R_T(k$\Omega \cdot cm^2$)	I_{SC}($\mu A \cdot cm^{-2}$)
NaS-R	−47 ± 5(6)	0.92 ± 0.02(6)	5 ± 1(6)	5.2 ± 0.6(6)
KS-R	−10 ± 3(6)	0.94 ± 0.01(6)	4 ± 1(6)	1.4 ± 0.3(6)
NaS-R	−49 ± 5(6)	0.91 ± 0.01(6)	5 ± 1(6)	5.2 ± 0.6(6)
NaS-R + mucosal amiloride	−74 ± 4(4)	0.930 ± 0.004(3)	6 ± 2(4)	0.7 ± 0.2(4)

The numbers in parentheses refer to the numbers of preparations included in the calculations.

was clearly reduced by high serosal K^+, it remained significantly greater than zero. This fact dictates (as illustrated by the graphs of Fig. 13) that the dependence of transepithelial current on apical membrane potential cannot be derived solely from measurements of transepithelial potential and current, even in the presence of serosal K_2SO_4-Ringer's solution.

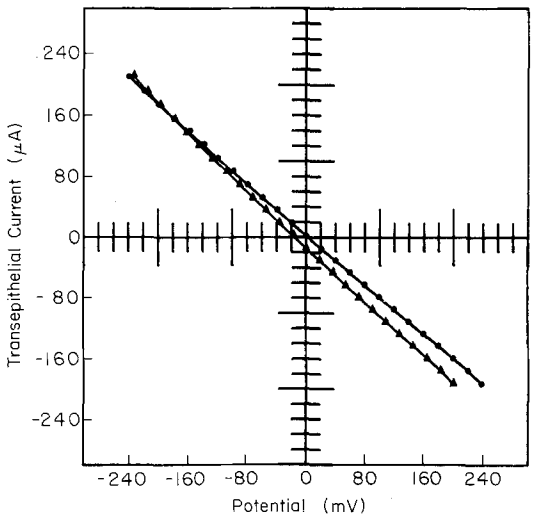

Fig. 13. Transepithelial current as a function of transepithelial potential (circles) and apical membrane potential (triangles) in a tissue bathed with high serosal K^+. The mucosal and serosal media were NaS-R and KS-R, respectively. The data were obtained 4 msec after the onset of each voltage pulse

Discussion

Capacitative Transients

The basic strategy of the present work has been to measure the electrophysiological parameters of frog skin epithelium as rapidly as possible after applying each transepithelial voltage pulse. This approach has been chosen in an effort to characterize the plasma membrane in the baseline state before substantial time- and voltage-dependent changes induced by the voltage pulses have had sufficient time to appear. This strategy is limited only by the capacitative transients induced in the transepithelial current (I_T) and apical membrane potential (ψ^{mc}). In the present study, analysis was practicable very soon after initiating each voltage pulse because of the short time constant τ of 1.35 ± 0.09 msec observed to characterize the epithelia studied.

Capacitative transients across frog skin epithelium can be analyzed within the framework of the equivalent circuit of Fig. 5*A* (Appendix). The time courses of apical membrane potential and transepithelial current following a positive step change in ψ^{ms} ($\varepsilon > 0$) are described by:

$$\psi^{mc} = \psi_o^{mc} + \left[\frac{\varepsilon}{1 + (R_b/R_a)}\right] + \left[\frac{1}{1 + (C_a/C_b)} - \frac{1}{1 + (R_b/R_a)}\right] e^{-t/\tau} \quad (17A)$$

$$I = I_o - [\varepsilon/(R_a + R_b)] - (\varepsilon C_a e^{-t/\tau}) \left[\frac{1}{1 + (C_a/C_b)} - \frac{1}{1 + (R_b/R_a)}\right]\left(\frac{1}{\tau_a} - \frac{1}{\tau}\right) \quad (19A)$$

where ψ_o^{mc} and I_o are the values of ψ^{mc} and I, respectively, just prior to the transepithelial voltage step. The time constant τ is defined by:

$$1/\tau = [1/(C_a + C_b)][(1/R_a) + (1/R_b)]. \quad (11A)$$

The time constant of the apical membrane alone (given by R_aC_a) is symbolized by τ_a in Eq. (19A). Eqs. (11A), (17A) and (19A) are instructive in two ways. First, they permit estimation of τ. Second, they indicate that additional information may be derived from the qualitative time course of apical membrane potential.

Taking the capacitances of the apical (C_a) and basolateral (C_b) membranes each to be 1 $\mu F \cdot cm^{-2}$, introduction of the measured values of R_a and R_b into Eq. (11A) leads to a mean estimated value for τ of 2.6 ± 0.7 msec. The mean ratio of measured-to-calculated values of τ was 0.8 ± 0.3 msec. It should be appreciated that the calculations of τ are open to

considerable uncertainty. Under certain conditions, the apical fractional resistance estimated as the ratio of the apical voltage change to the voltage step induced across the entire epithelium may underestimate the true value of f_o^{ap} (Nagel, Garcia-Diaz & Essig, 1983); this would lead to a falsely low experimental estimate of the basolateral conductance (Eq. 2) and a falsely high estimate of τ (Eq. 11A).

As pointed out by Schultz et al.,[1] the values of C_a and C_b are particularly uncertain; a wide range of estimates have been published. For example, taking C_a to be 1.6 $\mu F \cdot cm^{-2}$ and C_b to be 78 $\mu F \cdot cm^{-2}$ as estimated by Smith (1971), application of expression (11A) leads to a value of τ two orders of magnitude larger than that calculated above. These estimates of membrane capacitance appear entirely inapplicable to our tissues, not only because of the quantitative time-dependences of ψ^{mc} and I_T, but from a qualitative consideration, as well. As will be appreciated from Eq. (17A), following a positive voltage step ε in ψ^{ms}, the transient response in ψ^{mc} can be either greater or less than the steady-state deflection, depending upon the sign of the factor $\left[\frac{1}{1 + (C_a/C_b)} - \frac{1}{1 + (R_b/R_a)}\right]$. Assuming $C_a = 1.6$ $\mu F \cdot cm^{-2}$ and $C_b = 78$ $\mu F \cdot cm^2$ would lead to the conclusion that τ_a is much smaller than the time constant (τ_b) of the basolateral membrane (given by R_bC_b). Under this condition, the above factor of Eq. (17A) would be positive. Hence, the transient deflection of the apical membrane potential would be greater than the steady-state value (curve 3 of Fig. 4*B*), contrary to observation.

As pointed out in the Appendix, Eq. (17A) is particularly instructive in emphasizing that the transient in ψ^{mc} can be positive or negative, depending upon the relative magnitudes of τ_a and τ_b. In the special circumstance that $\tau_a = \tau_b$, ψ^{mc} should exhibit squarewave behavior, even when the time constant for the entire skin is very long.

Applicability of Goldman Equation

The aim of the present study has been to address two questions: (i) Can the relationship between membrane potential (ψ^{mc}) and sodium current (I_{Na}) across the apical membrane of frog skin epithelium be fit by the constant field equation, and (ii) can application of high serosal K^+ permit the rigorous determination of the I_{Na}-ψ^{mc} relationship across frog skin epithelium solely by transepithelial measurements. The results of the current work provide unequivocal answers to both questions.

Figures 9–11 document that the Goldman equation provides an excellent fit of the I_{Na}-ψ^{mc} relationship over apical voltage ranges of 300 to 420 mV in each and every one of the five successful complete experiments. This result is similar to that reported by Thompson, Suzuki and Schultz (1982) for rabbit descending colon and by Thomas et al. (1983) for *Necturus* urinary bladder. The fit is, in fact, so remarkably good as to raise the question why previous reports have described fits over far more limited voltage ranges (Fuchs, Larsen & Lindemann, 1977; from $\psi^{mc} = 0$ to $\psi^{mc} < 80$ mV) or have found no consistent fit at all (at least in preliminary experiments; Helman, 1981; Tang & Helman, 1982). Although a definitive answer is not possible from the current data alone, at least five factors may have played a role in obscuring the excellence of the fit.

First, species and subspecies differences, and the use of the isolated epithelium rather than whole skin may possibly have contributed to the differences observed. Second, Fuchs, Larsen and Lindemann used lower mucosal concentrations of Na^+. There is some suggestion in the published literature that agreement with the Goldman equation is observed over a wider range of apical membrane potentials at higher mucosal concentrations (Thomas et al., 1983, their Fig. 8). Third, the duration of the pulses used, and the choice of constant current or constant voltage pulses is clearly important. For example, Frömter et al. (1981) used an endpoint of 200 msec after initiating constant current pulses across *Necturus* urinary bladder, and found a satisfactory fit over an apical voltage range only about a third as great as that observed by Thomas et al. (1983), who used an endpoint of 16 msec after initiating constant voltage pulses. The potential importance of choosing very early endpoints in time is also strongly suggested by the present data. For example, inspection of the deflections in ψ^{sc} in Fig. 1 in response to 10-mV hyperpolarizations of ψ^{ms} might suggest that the basolateral fractional resistance is as large as 0.25. Closer inspection of the trace, however, indicates that the initial deflection of ψ^{sc} is much smaller than that noted after several seconds. Using an endpoint of 8 msec (7.5 msec after the rapid transient response had been completed in this preparation), f_o^{bl} was actually found to be only 0.06. The complexities and one possible basis for the voltage and current transients across anuran tight epithelia over periods of seconds have been discussed elsewhere (Weinstein et al., 1980). It will be appreciated that even over the very narrow time interval of 1 to 25 msec, small changes in the I_{Na}-ψ^{mc} relationship can be noted (Fig. 11).

A fourth factor which may influence the fit of the measurements to the Goldman equation is the choice of pulsing sequence. For example, Fuchs et al. (1977) used a staircase sequence in their impor-

tant seminal study. Insofar as the epithelial electrophysiological properties are both voltage- and time-dependent, we consider it more prudent to return ψ^{mc} to the initial holding voltage following each voltage step (e.g., Civan, 1970; Helman & Fisher, 1977; Thompson, Suzuki & Schultz, 1982). In the present study, one criterion for data acceptability was the requirement that ψ_o^{sc} return to within 2 mV of the prepulse value following each voltage pulse across the epithelium.

A fifth important factor which must affect the fit to the constant field equation is the choice of transepithelial or transmembrane measurements in estimating the I_{Na}-ψ^{mc} relationship. This issue requires examination of two questions. Does the application of high serosal concentrations of K^+ leave the transport properties of the epithelium largely unchanged? Whether or not the skin is in a different transport state, are the current-voltage relationships generated by measurements of ψ^{ms} and of ψ^{mc} identical?

Use of Depolarized Preparation

Several lines of evidence suggest that high serosal potassium significantly changes the transport state of isolated epithelia. Cuthbert and Wilson (1981) have noted that high external potassium concentrations produce a marked increase in cyclic 3′,5′-AMP formation. High serosal potassium has been found to reduce the apical Na^+ permeability of rabbit colon by some 40% (Thomas, Suzuki & Schultz, 1981; their Table 2). High serosal potassium may also alter the dependence of intracellular Na^+ activity upon mucosal Na^+ activity in the short-circuited *Necturus* urinary bladder (Thomas et al., 1983; their footnote 5). In the present study, the quantitative substitution of serosal K^+ for Na^+ markedly lowered the transepithelial current at a transepithelial potential of zero.

The issue of the identity of transmembrane and transmural measurements in the presence of high serosal potassium has been less clear until now. In this condition, ψ_o^{sc} has been found indistinguishable from zero in rabbit descending colon (Thompson, Suzuki & Schultz, 1981) and in nystatin- or amphotericin-treated frog skins bathed with sulfate-, but not chloride-Ringer's solution (Benos, Hyde & Latorre, 1983). However, Nagel (1977, 1979) and Tang and Helman (1983) have reported that ψ_o^{sc} may be as much as 20 to 30 mV different from zero in frog skin, and Lewis, Wills and Eaton (1978) have noted a difference of 10 to 15 mV in rabbit urinary bladder. The data from the present study indicate that the deviation from zero can be variable from skin to skin. In three epithelial preparations, the assumption that $\psi_o^{sc} = 0$ was not an unreasonable approximation. In three others, the approximation was clearly incorrect.

The possibility must be considered that the measured deviations of ψ_o^{sc} from zero in the presence of high serosal K^+ might conceivably reflect only junction and tip potentials. This possibility seems highly unlikely from both experimental and theoretical considerations. The intracellular measurements of the present work were reproducible in a given preparation, stable over periods of many minutes (Figs. 1 and 12), and conformed to commonly applied criteria of acceptability (DeLong & Civan, 1983*a*). In addition, each and every determination of ψ_o^{sc} in the presence of serosal KS-R was associated with a hyperpolarization following restoration of serosal Na^+ (Fig. 12). The use of 0.5 M KCl as a filling solution reduced the potential problem of saline diffusion into the impaled cell (Nelson et al., 1978; Fromm & Schultz, 1981). Penetrations across the basolateral rather than apical membranes minimized impalement-induced polarizations (Higgins et al., 1977), and eliminated any possibility of artifact associate with impalements through the *stratum corneum*.

Actually, it is very likely that the measured values of ψ_o^{sc} of -3 to -19 mV appreciably underestimated the true residual membrane polarizations for skins bathed with high serosal K^+. The results of impalements of *Chironomus* salivary glands by Palmer and Civan (1977) using micropipettes containing different filling solutions support the applicability of the Henderson equation for calculating the liquid junction potential (ϕ). DeLong and Civan (1983*a*) have estimated ϕ to be 7.3 mV for a 0.5 M KCl-filled micropipette relative to the intracellular fluid of frog skin under baseline conditions, so that the corrected estimates of ψ_o^{sc} should be about -10 to -25 mV. Given this significant and variable membrane potential and the finite residual basolateral membrane resistance (Fig. 13), calculation of the I_{Na}-ψ^{mc} relationship solely from transepithelial measurements is, in general, unjustified.

It should be appreciated that it may well be possible to find experimental conditions (different species or subspecies of frog, different bathing solutions, different periods of preincubation with high serosal K^+) where the I_{Na}-ψ^{mc} and I_{Na}-ψ^{ms} relationships are identical. However, such an identity cannot be assumed *a priori* and should be documented for each experimental condition. On the other hand, in those preparations (such as the urinary bladder of the toad) where stable reproducible records of membrane potential (such as those of Figs. 1 and 12) are not technically feasible, the approach of

Fuchs et al. (1977) may provide a useful approximation of the true I_{Na}-ψ^{mc} relationship under more physiologic conditions. This conclusion is not very different from that reached by Palmer (1984) in his recent useful review.

Significance of Fitting to Constant Field Equation

The applicability of the Goldman equation to apical Na^+ entry across frog skin is helpful in at least two ways. First, the adequacy of fit is of some limited theoretical value, supporting the concept of electrodiffusive Na^+ entry. As noted by others (Stark, 1973; Frömter et al., 1981; Schultz et al., 1981), a similar I_{Na}-ψ^{mc} relationship can be generated by nonelectrodiffusive mechanisms. In fact, the principal evidence in favor of electrodiffusive apical entry of Na^+ is the very high rate of turnover of Na^+ ($\sim 10^6$ sec^{-1}) at the translocation sites in frog skin (Lindemann & Van Driessche, 1977) and the urinary bladder of the toad (Li et al., 1979); this rate has been thought far faster than the maximal likely rate of carrier-mediated transport (Armstrong, 1975*a*,*b*). Furthermore, it should be appreciated that inapplicability of the Goldman equation, *per se*, would not necessarily be incompatible with electrodiffusive entry, but could instead reflect a more complex energy potential profile across the membrane than that assumed by the constant field equation (e.g., Benz & McLaughlin, 1983).

The second and more immediately valuable use of fitting the Goldman equation to the electrophysiologic data lies in obtaining quantitative descriptive information concerning both the intracellular Na^+ activity and the entry sites themselves (permeability, chord conductance and slope conductance). The data of Table 3 provide the basis for two points of comparison with published results obtained by different techniques. The estimates of intracellular Na^+ have been expressed in units of concentration (c^c_{Na}), assuming constancy of the activity coefficient for Na^+ inside and outside the cell; the results could also have been expressed in terms of activity without that assumption. Neglecting the junction potential, c^c_{Na} is estimated to be 7 to 10 mM, depending upon the endpoint used. When correction is made for the junction potential, c^c_{Na} is calculated to be 9 to 14 mM. This range of values is remarkably similar to the estimates of $c^c{}_{Na}$ which can be calculated from results obtained by electron probe X-ray microanalysis of frog skins similarly bathed with identical Ringer's solution on their two surfaces and containing a Na^+ concentration of 110 mM (similar to that of the present study) (Rick et al., 1978). Under control conditions, the intracellular Na^+ concentration of cells in the *strata granulosum, spinosum* and *germinativum* ranged from 6.4 to 14.4 mmol · kg wet weight^{-1} in individual skins, with a mean of 9.4 mmol · kg wet weight^{-1}. Using their reported estimate of 0.254 for the fractional dry weight of the cytoplasm, these values correspond to Na^+ concentrations ranging from 8.6 to 19.3, with a mean of 12.4, when expressed in mM.

The data of Table 2 also provide us with another index for assessing the adequacy of models of Na^+ transport across frog skin. Using data points corrected for junction potential, P^{ap}_{Na} is calculated to be 4.7 to 5.0 $\times$ 10^{-7} cm^3 · sec^{-1} for skins 1.9 cm^2 in area, equivalent to 2.5 to 2.6 $\times$ 10^{-7} cm · sec^{-1}. This permeability agrees within a factor of 3 with the estimate generated by the theoretical model of Lew, Ferreira and Moura (1979) and within a factor of 4 generated by a modification of that model (Civan & Bookman, 1982; Civan, 1983).

We thank Dr. George M. Fanelli, Jr. (Merck Institute for Therapeutic Research, West Point, Pa.) for generously providing us with samples of amiloride and Dr. Stephen M. Thompson in communicating the details of the computer program used by Thompson, Suzuki and Schultz (1981), although their program was not, in fact, used in the present study. We are grateful to Mrs. Kim Peterson-Yantorno for her extremely skillful technical assistance, and to Drs. Clay M. Armstrong and Stanley G. Schultz for helpful and stimulating discussions concerning our analysis of capacitative transients. This work was supported in part by a research grant from the National Institutes of Health (AM 20632).

References

Armstrong, C.M. 1975*a*. Evidence for ionic pores in excitable membranes. *Biophys. J.* **15**:932–933

Armstrong, C.M. 1975*b*. Ionic pores, gates and gating currents. *Q. Rev. Biophys.* **7**:179–210

Benos, D.J., Hyde, B.A., Latorre, R. 1983. Sodium flux ratio through the amiloride-sensitive entry pathway in frog skin. *J. Gen. Physiol.* **81**:667–685

Benz, R., McLaughlin, S. 1983. The molecular mechanism of action of the proton ionophore FCCP (carbonylcyanide *p*-trifluoromethoxyphenylhydrazone). *Biophys. J.* **41**:381–398

Carasso, N., Favard, P., Jard, S., Rajerison, R.M. 1971. The isolated frog skin epithelium: I. Preparation and general structure in different physiological states. *J. Microsc. (Paris)* **10**:315–330

Civan, M.M. 1970. Effects of active sodium transport on current-voltage relationship of toad bladder. *Am. J. Physiol.* **219**:234–245

Civan, M.M. 1983. Epithelial Ions and Transport: Application of Biophysical Techniques. Wiley, New York

Civan, M.M., Bookman, R.J. 1982. Transepithelial Na^+ transport and the intracellular fluids: A computer study. *J. Membrane Biol.* **65**:63–80

Civan, M.M., Peterson-Yantorno, K., DiBona, D.R., Wilson,

D.F., Erecińska, M. 1983. Bioenergetics of Na^+ transport across frog skin: Chemical and electrical measurements. *Am. J. Physiol.* **245:**F691–F700

Cuthbert, A.W., Wilson, S.A. 1981. Mechanisms for the effects of acetylcholine on sodium transport in frog skin. *J. Membrane Biol.* **59:**65–75

DeLong, J., Civan, M.M. 1978. Dissociation of cellular K^+ accumulation from net Na^+ transport by toad urinary bladder. *J. Membrane Biol.* **42:**19–43

DeLong, J., Civan, M.M. 1983*a*. Microelectrode study of K^+ accumulation by tight epithelia: I. Baseline values of split frog skin and toad urinary bladder. *J. Membrane Biol.* **72:**183–193

DeLong, J., Civan, M.M. 1983*b*. Microelectrode study of K^+ accumulation by tight epithelia: II. Effect of inhibiting transpithelial Na^+ transport on reaccumulation following depletion. *J. Membrane Biol.* **74:**155–164

Fisher, R.S., Erlij, D., Helman, S.I. 1980. Intracellular voltage of isolated epithelia of frog skin: Apical and basolateral cell punctures. *J. Gen. Physiol.* **76:**447–453

Fromm, M., Schultz, S.G. 1981. Some properties of KCl-filled microelectrodes: Correlation of potassium "leakage" with tip resistance. *J. Membrane Biol.* **62:**239–244

Frömter, E., Higgins, J.T., Gebler, B. 1981. Electrical properties of amphibian urinary bladder epithelia. IV. The current-voltage relationship of the sodium channels in the apical cell membrane. *In:* Ion Transport by Epithelia. S.G. Schultz, editor. pp. 31–45. Raven, New York

Fuchs, W., Larsen, E.H., Lindemann, B. 1977. Current-voltage curve of sodium channels and concentration dependence of sodium permeability in frog skin. *J. Physiol. (London)* **267:**137–166

Goldman, D.E. 1943. Potential, impedance and rectification in membranes. *J. Gen. Physiol.* **27:**37–60

Helman, S.I. 1981. Electrical rectification of the sodium flux across the apical barrier of frog skin epithelium. *In:* Ion Transport by Epithelia. S.G. Schultz, editor. pp. 15–30. Raven, New York

Helman, S.I., Fisher, R.S. 1977. Microelectrode studies of the active Na transport pathway of frog skin. *J. Gen. Physiol.* **69:**571–604

Higgins, J.T., Jr., Gebler, B., Frömter, E. 1977. Electrical properties of amphibian urinary bladder epithelia. II. The cell potential profile in *Necturus maculosus*. *Pfluegers Arch.* **371:**87–97

Koefoed-Johnsen, V., Ussing, H.H. 1958. The nature of the frog skin potential. *Acta Physiol. Scand.* **42:**298–308

Lew, V.L., Ferreira, H.G., Moura, T. 1979. The behaviour of transporting epithelial cells. I. Computer analysis of a basic model. *Proc. R. Soc. London, B* **206:**53–83

Lewis, S.A., Eaton, D.C., Diamond, J.M. 1976. The mechanism of Na^+ transport by rabbit urinary bladder. *J. Membrane Biol.* **28:**41–70

Lewis, S.A., Wills, N.K., Eaton, D.C. 1978. Basolateral membrane potential of a tight epithelium: Ion diffusion and electrogenic pumps. *J. Membrane Biol.* **41:**117–148

Li, J.H.-Y., Palmer, L.G., Edelman, I.S., Lindemann, B. 1982. The role of sodium-channel density in the natriferic response of the toad urinary bladder to an antidiuretic hormone. *J. Membrane Biol.* **64:**77–89

Lichtenstein, N.S., Leaf, A. 1965. Effect of amphotericin B on the permeability of the toad bladder. *J. Clin. Invest.* **44:**1328–1342

Lindemann, B., Van Driessche, W. 1977. Sodium specific membrane channels of frog skin are pores: Current fluctuations reveal high turnover. *Science* **195:**292–294

Nagel, W. 1977. Effect of high K upon the frog skin intracellular potential. *Pfluegers Arch.* **368:**R22

Nagel, W. 1979. Inhibition of potassium conductance by barium in frog skin epithelium. *Biochim. Biophys. Acta* **552:**346–357

Nagel, W., Garcia-Diaz, J.F., Essig, A. 1983. Contribution of junctional conductance to the cellular voltage-divider ratio in frog skin. *Pfluegers Arch.* **399:**336–341

Nelson, D.J., Ehrenfeld, J., Lindemann, B. 1978. Volume changes and potential artifacts of epithelial cells of frog skin following impalement with microelectrodes filled with 3 M KCl. *J. Membrane Biol.*, **Special Issue:**91–119

Palmer, L.G. 1984. Use of potassium depolarization to study apical transport properties in epithelia. *Curr. Top. Membr. Transp.* **20:**105–121

Palmer, L.G., Civan, M.M. 1977. Distribution of Na^+, K^+ and Cl^- between nucleus and cytoplasm in *Chironomus* salivary gland cells. *J. Membrane Biol.* **33:**41–61

Palmer, L.G., Edelman, I.S., Lindemann, B. 1980. Current-voltage analysis of apical sodium transport in toad urinary bladder: Effects of inhibitors of transport and metabolism. *J. Membrane Biol.* **57:**59–71

Palmer, L.G., Li, J.H.-Y., Lindemann, B., Edelman, I.S. 1982. Aldosterone control of the density of sodium channels in the toad urinary bladder. *J. Membrane Biol.* **64:**91–102

Rick, R., Dörge, A., Arnim, E. von, Thurau, K. 1978. Electron microprobe analysis of frog skin epithelium: Evidence for a syncytial sodium transport compartment. *J. Membrane Biol.* **39:**313–331

Schultz, S.G., Thompson, S.M., Suzuki, Y. 1981. On the mechanism of sodium entry across the apical membrane of rabbit colon. *In:* Epithelial Ion and Water Transport. A.D.C. Macknight and J.P. Leader, editors. pp. 285–295. Raven, New York

Smith, P.G. 1971. The low frequency electrical impedance of the isolated frog skin. *Acta Physiol. Scand.* **81:**355–366

Stark, G. 1973. Rectification phenomena in carrier-mediated ion transport. *Biochim. Biophys. Acta* **298:**323–332

Tang, J., Helman, S.I. 1982. Relationship between Na current and voltage at the apical membrane of frog skin. *Fed. Proc.* **41:**1349

Tang, J., Helman, S.I. 1983. Electrical parameters of apical and basolateral membranes of *R. pipiens* depolarized by 100 mM $[K]_o$. *Fed. Proc.* **42:**1101

Thomas, S.R., Suzuki, Y., Thompson, S.M., Schultz, S.G. 1983. Electrophysiology of *Necturus* urinary bladder: I. "Instantaneous" current-voltage relations in the presence of varying mucosal sodium concentrations. *J. Membrane Biol.* **73:**157–175

Thompson, S.M., Suzuki, Y., Schultz, S.G. 1981. Current-voltage properties of the active sodium transport pathway across rabbit colon. *In:* Ion Transport by Epithelia. S.G. Schultz, editor. pp. 47–59. Raven, New York

Thompson, S.M., Suzuki, Y., Schultz, S.G. 1982. The electrophysiology of rabbit descending colon: II. Current-voltage relations of the apical membrane, the basolateral membrane, and the parallel pathways. *J. Membrane Biol.* **66:**55–61

Weinstein, F.C., Rosowski, J.J., Peterson, K., Delalic, Z., Civan, M.M. 1980. Relationship of transient electrical properties to active sodium transport by toad urinary bladder. *J. Membrane Biol.* **52:**25–35

Received 13 January 1984; revised 10 April 1984

Appendix

Figure 4 provides an equivalent circuit for analyzing the amiloride-sensitive transcellular pathway during the course of a step change in transepithelial voltage from $\psi^{ms} = 0$ to $\psi^{ms} = \varepsilon$. The subscripts "a" and "b" refer to the equivalent circuit elements at the apical and basolateral membranes, respectively. The subscript "o" refers to the steady-state value in the short-circuited state ($\psi^{ms} = 0$). The superscripts "m", "c" and "s" refer to the mucosal, intracellular and serosal phases, respectively. The fundamental definitions and equations for analysis are:

$$\psi^{ms} \equiv \psi^s - \psi^m \tag{1A}$$

$$\psi^{cs} \equiv \psi^s - \psi^c \tag{2A}$$

$$\psi^{mc} \equiv \psi^c - \psi^m \tag{3A}$$

$$I_o = (E_a + E_b)/(R_a + R_b) \tag{4A}$$

$$\psi_o^{mc} = E_a - I_o R_a \tag{5A}$$

$$\psi_o^{cs} = E_b - I_o R_b \tag{6A}$$

$$I = [(E_b - \psi^{cs})/R_b] - \dot{\psi}^{cs} C_b \tag{7A}$$

$$I = [E_a - \psi^{mc})/R_a] - \dot{\psi}^{mc} C_a \tag{8A}$$

where the symbol "$\cdot$" denotes the time derivative of the function.

$$\psi^{cs} = \varepsilon - \psi^{mc} \tag{9A}$$

$$\dot{\psi}^{cs} = -\dot{\psi}^{mc} \tag{10A}$$

$$1/\tau \equiv [1/(C_a + C_b)][(1/R_a) + (1/R_b)] \tag{11A}$$

$$(\psi_\infty^{mc}/\tau) \equiv [1/(C_a + C_b)][(E_a/R_a) - (E_b/R_b) + (\varepsilon/R_b)] \tag{12A}$$

$$\therefore \dot{\psi}^{mc} + \psi^{mc}(1/\tau) = \psi_\infty^{mc}/\tau \tag{13A}$$

$$\therefore \psi^{mc} = \psi_\infty^{mc} + (\psi_i^{mc} - \psi_\infty^{mc}) e^{-t/\tau} \tag{14A}$$

where ψ_i^{mc} is the initial value of ψ^{mc} immediately after the step change in ψ^{ms}, and the subscript "∞" refers to the steady-state value. Taking into account that the step change in ψ^{ms} is very rapid (~0.5 msec), ψ_i^{mc} can be estimated from Fig. 4. Under these circumstances, the conductance component ($1/R$) of the admittance presented by each membrane to the high frequency components of the applied voltage is negligibly small in comparison to the susceptance (ωC), where ω is the angular frequency of the Fourier voltage component. Therefore, the applied voltage step (ε) will produce the same displacement current through each of the capacitances, C_a and C_b; the fraction of ε appearing instantaneously across each membrane barrier will be inversely proportional to the capacitance of that barrier:

$$\psi_i^{mc} = \psi_o^{mc} + \left[\varepsilon \Big/ \left(1 + \frac{C_a}{C_b}\right)\right]. \tag{15A}$$

From Eqs. (14A) and (15A),

$$\psi^{mc} = \psi_\infty^{mc} + \left[\psi_o^{mc} + \frac{\varepsilon}{1 + (C_a/C_b)} - \psi_\infty^{mc}\right] e^{-t/\tau}. \tag{16A}$$

From Eqs. (5A), (12A) and (16A), the apical membrane potential can also be expressed as:

$$\psi^{mc} = \psi_o^{mc} + \left[\frac{\varepsilon}{1 + (R_b/R_a)}\right] + \varepsilon \left[\frac{1}{1 + (C_a/C_b)} - \frac{1}{1 + (R_b/R_a)}\right] e^{-t/\tau}. \tag{17A}$$

Differentiating Eq. (17A),

$$\dot{\psi}^{mc} = -(\varepsilon/\tau)\left[\frac{1}{1 + (C_a/C_b)} - \frac{1}{1 + (R_b/R_a)}\right] e^{-t/\tau}. \tag{18A}$$

From Eqs. (4A), (8A), (17A) and (18A),

$$I = I_o - \left(\frac{\varepsilon}{R_a + R_b}\right) - (\varepsilon C_a e^{-t/\tau}) \left[\frac{1}{1 + (C_a/C_b)} - \frac{1}{1 + (R_b/R_a)}\right]\left[\frac{1}{\tau_a} - \frac{1}{\tau}\right] \tag{19A}$$

where

$$\tau_a \equiv R_a C_a. \tag{20A}$$

The time courses of ψ^{mc} and I predicted by Eqs. (17A) and (19A), respectively, are presented in the idealized cartoons of Fig. 4*B*. As emphasized in the Figure, three possible time courses are predicted by Eq. (17A) for the apical membrane potential following a step change in the transepithelial clamping voltage. If $\tau_a > \tau_b$, the factor

$$\left[\frac{1}{1 + (C_a/C_b)} - \frac{1}{1 + (R_b/R_a)}\right]$$

of Eq. (17A) is negative leading to the time course of curve 1. If $\tau_a < \tau_b$, the argument is positive, resulting in trajectory 3. If $\tau_a = \tau_b$, the apical membrane potential is expected to exhibit squarewave behavior, independent of the absolute value of τ.

As illustrated by Fig. 4*B*, the time course of I predicted by Eq. (19A) is simpler than that for ψ^{mc} since the factors

$$\left[\frac{1}{1 + (C_a/C_b)} - \frac{1}{1 + (R_b/R_a)}\right]$$

and $(1/\tau_a - 1/\tau)$ are always the same in sign. Where $\tau_a > \tau_b$, both are negative and when $\tau_a < \tau_b$, both are positive. In either case, the step change in ψ^{ms} elicits a brief surge of current, producing the initial charges on C_a and C_b, following which I decays exponentially to its steady-state value. However, as for ψ^{mc}, when $\tau_a = \tau_b$, I displays a squarewave response following the brief surge current.